Frequencies of multivariate air masses drive global tree growth

Cameron C. Lee*[1,2]
Matthew P. Dannenberg[3]

[1] – Kent State University; Department of Geography
[2] – Kent State Environmental Science and Design Research Institute
[3] – University of Iowa; Department of Geographical and Sustainability Sciences

* – Corresponding Author
Kent State University
325 S. Lincoln St.
433 McGilvrey Hall
Kent, Ohio 44242 USA
Phone: +1 330-672-0360
Email: cclee@kent.edu

KEY POINTS:

- Global tree-ring widths are significantly related to variability in synoptic-scale air mass frequency in the year preceding growth
- The most important air masses are dry, dry-warm, and humid-cool air masses, especially in relatively hot locations
- At about 60% of sites and for 83% of well-sampled species, air mass models outperform models based on temperature and precipitation alone

ABSTRACT:
Surface meteorological conditions in the midlatitudes are embedded within and affected by synoptic-scale systems, including the movement and persistence of air masses (AMs). Changes in the frequencies of different AMs over the past several decades could potentially have large effects on ecosystems: each organism is exposed to the synergistic effects of the entire suite of atmospheric variables acting upon it – an inherently multivariate environment – which is best captured using AMs. Utilizing a global-scale AM classification system and a global network of tree-ring widths, we investigate how variation in AM frequency impacts tree growth at over 900 locations. We find that AM frequencies are well-correlated with tree growth, especially in the 12-month period from July in the year prior to growth through June in the year of growth. The most important AMs are Dry-Warm and Humid-Cool AMs, which exhibit average correlations of ρ=-0.4 and ρ=+0.4 with global tree growth, respectively, among commonly sampled tree species, with correlations at some sites exceeding ρ=+/-0.8 in some seasons. Compared to empirical models based solely on temperature and precipitation, modeling using only AM frequencies proved superior at nearly 60% of the sites and for over 80% of the well-sampled ($n \geq 10$) species. These results should provide a foundation for using AMs to improve forecasts of tree growth, tree stress and wildfire potential. Long-term reconstructions of AM frequencies back several centuries may also be feasible using tree-ring data, which will help contextualize and temporally extend multivariate perspectives of climate change that utilize such air masses.

PLAIN LANGUAGE SUMMARY:
Tree-ring widths depend on the weather a particular tree experiences, and are a direct indicator of tree growth and tree health. Most often, the relationship between tree rings and weather are described using temperature, precipitation, or drought indices. However, a tree is exposed not just to temperature and/or precipitation alone, but to all weather elements acting together, which can be defined using air masses (AMs). In this research, we explore how AMs impact tree growth at over 900 locations around the world. We find that tree-ring widths are significantly related to the frequency of certain AMs, especially Dry and Warm air masses and Humid and Cool air masses. Further, we find that air masses often affect tree growth more than temperature and precipitation alone, up to a year prior to when the tree ring grew. Air mass information could therefore aid in forecasting tree/forest health and in predicting wildfire potential.

KEYWORDS: synoptic climatology, climate variability, climate change, tree rings, dendroclimatology, ecological forecasting

1. INTRODUCTION AND BACKGROUND

Variability in mid-latitude surface weather is largely controlled by the ridges and troughs embedded in the hemispheric-scale circulation of the polar front jet stream, and the movement and persistence of accompanying synoptic-scale air masses (AMs). Significant trends in AM frequencies have occurred over the last several decades (Lee, 2020a; Petrou et al. 2022), with general increases in warm-type AMs at the expense of cold-type AMs (Lee & Sheridan, 2018). However, the instrumental and reanalysis record of atmospheric circulation and near-surface weather (on which AM classifications depend) generally cover only the past half-century, and recent trends in AM frequencies must still be contextualized within a multi-century climate history. Variability in AM frequencies at different time scales can also have wide-ranging impacts on various systems (e.g. Hondula et al., 2012, Lee 2015a; Labosier et al., 2015). However, their collective effects on the growth and productivity of ecological systems remain largely unknown. While most bioclimatological research examines univariate relationships between individual meteorological variables (especially temperature and precipitation) and ecological systems of interest, using air masses as the unit of analysis captures the wholistic, "multivariate environment" to which an organism is exposed. That is, temperature and/or precipitation do not act in isolation upon an organism (or ecosystem), but rather each individual is exposed to the *synergistic* effects of the entire suite of atmospheric components acting upon it, which are well captured by AM frequencies.

Tree rings provide the means both to evaluate the impact of climate on forest growth and productivity ("climate response," e.g., Dannenberg et al., 2019, 2020; Kannenberg et al., 2019a; Peltier et al., 2018; Williams et al., 2013) and, given that many tree species can live for hundreds or even thousands of years, to reconstruct past climates ("climate reconstruction," e.g., Cook et al., 1999, 2015; Wilson et al., 2016; Wise, 2010, 2016). While much of this work has focused on either temperature or precipitation/drought, recent work in "synoptic dendroclimatology" (Hirschboeck et al., 1996) examines growth responses to synoptic-scale atmospheric circulation (Dannenberg & Wise, 2017; Hudson et al., 2019) and reconstructs those circulation patterns in the pre-instrumental period (Trouet et al., 2018; Wise & Dannenberg, 2014, 2017). While some studies have examined connections between synoptic-scale air masses and tree growth at regional scales (Schultz and Neuwirth, 2012; Seim et al., 2017; Senkbeil et al., 2007; Woodhouse & Kay, 1990), recent developments in air mass classification systems and further development of the global tree-ring database now allow global-scale assessment of the impacts of AM frequencies (and their lagged effects) on tree growth across many species and regions. Hence, a bioclimatological investigation relating tree rings and AM variability could yield not only new information on how AMs impact ecological systems but could also lay the groundwork for reconstructing past AM frequencies, allowing the comparison of recent trends in AM frequencies to pre-instrumental variability.

Here, we use tree-ring width records from over 900 sites (spanning over 140 species from 36 distinct genera) to examine the influence of seasonal AM frequencies on global tree growth. Specifically, we use correlation analysis to determine the magnitude and direction of the relationship between tree growth and the frequencies of 11 air masses in eight seasons – the four seasons in the year of growth, and the four seasons in the year prior to growth.

Additionally, we use machine learning to examine the potential for using seasonal AM frequencies to predict tree growth at global scales, comparing the predictive power to that achieved with similar models based on temperature and precipitation, which are more commonly-used for modeling tree-ring width (e.g., Anchukaitis et al., 2020; Dannenberg, 2021; Tolwinski-Ward et al., 2011, 2013). By establishing empirical relationships between tree growth and AM frequency, we aim to lay the groundwork for future research geared both towards forecasting tree growth prior to the start of the growing season and towards reconstruction of long-term historical AM frequencies, thereby extending recent research examining AM changes over the past several decades to a multi-century context.

2. DATA AND METHODS

2.1. Tree-ring data

We obtained global annual measurements of tree-ring width (TRW), along with site metadata, from the International Tree Ring Data Bank (ITRDB) for a total of 4349 sites. To the extent possible, we identified and corrected errors or gaps in the metadata (e.g., incorrectly formatted geographic coordinates or species codes). Using the dplR package (Bunn, 2008) in the R statistical computing environment (R Core Team, 2021), we detrended each individual TRW series using a smoothing spline 2/3 the length of the series (Cook & Peters, 1981), after which we developed standard site-level chronologies using Tukey's biweight robust mean of all detrended series at that site. Of the original 4349 tree-ring records in the database, only those that had end-dates between 2005 and 2020 (to maximize overlap with the short instrumental/AM record) and valid geographic coordinates were selected for further evaluation, leaving 939 sites (Figure 1). For each site, we also obtained monthly mean temperature and precipitation, along with mean annual temperature (MAT) and precipitation (MAP), from the nearest grid cell of the ~4 km TerraClimate dataset (Abatzoglou et al., 2018).

2.2. Air mass classification

We used version two of the Gridded Weather Typing Classification system (GWTC2) first developed by Lee (2015b) and upgraded by Lee (2020b). The GWTC2 was chosen over other air mass classification systems due to its availability in the fairly rural locations from which tree-ring data largely come, and its global scope. The GWTC uses gridded reanalysis (at 0.5° x 0.5° spatial resolution) and model initialization data from the U.S. National Oceanic and Atmospheric Administration's Climate Forecast System (CFS) to identify daily-scale, near-surface air masses (also known as "weather types") for about 260,000 locations across the globe, 1979-present. Air masses are defined using 3-hourly (8-times daily) values of 2-m temperature, 2-m dew point, sea-level pressure, 10-m wind speed and wind direction [derived from zonal (u) and meridional (v) wind components] and total column cloud cover percentages. Through a multi-stage process (described in detail in Lee, 2015b; 2020b), the GWTC2 classifies every day at every location into one of 11 different air masses (Figure 2). The 9 'core' GWTC air masses partition temperature and humidity into 3 categories each; from concurrently humid and cool (HC) weather to concurrently dry and warm (DW) weather on one diagonal axis, and from concurrently humid and warm (HW) to concurrently

dry and cool (DC) weather on the opposite axis. Since not every day fits into a single designated category, there are also two 'transitional' air masses – cold front passage (CFP) and warm front passage (WFP) – that identify days on which the weather could more aptly be defined as changing from one air mass to another, much like what would be experienced during frontal passages. These air masses are both seasonally and geographically relative, meaning that, for example, a HW day can/does occur in January in Greenland because HW simply indicates that relative to that specific time of year and specific location (i.e. relative to all Januaries in Greenland) that day was warmer and more humid than normal. In the center of the 9 core air masses (in Figure 2) is the Seasonal (S) AM, which indicates a 'typical' weather day for a location/season and makes up ~30% of all days at most locations. The entire GWTC2 dataset is publicly and freely available, updated monthly, and provides real-time 60-day forecasts (at https://www.personal.kent.edu/~cclee/gwtc2global.html).

2.3. Statistical analysis

For each of the 939 retained tree-ring sites, the nearest land-based coordinate of the GWTC2 dataset was selected as its matched AM data. The TRW data and matched AM data were then trimmed to match overlapping years. For example, if the TRW data went from 1832 to 2012, it was trimmed to 1979 to 2012 to match the GWTC data that starts in 1979. Daily frequencies of each AM at that location were then summed by calendar quarter/season (JFM, AMJ, JAS, OND). These seasonal AM frequency counts were the basis of all analyses.

To examine each individual AM's relationship to tree-ring width, we used Spearman-rank correlation analysis (ρ). These correlations were computed for each of the 11 air mass frequency counts for each of the 4 seasons of the year corresponding to the year of tree growth (Year0) and for the year prior to growth (Year -1; i.e. how well the prior-year's AM frequencies in each of the 4 quarters correlated with the following year's TRW), thus yielding a total of n=88 (11 air masses x 4 seasons x 2 years) correlations computed for each of the 939 retained tree-ring records.

To quantify variability in tree-ring width explained by all AMs collectively, we trained cascade-forward artificial neural network (ANN) models for each of the 939 records. These ANNs were trained to learn annual TRW based upon the standardized summed counts of each AM occurrence in the 12-month period between July of Year -1, and June of Year0 (which was shown to be the key time period relating to TRWs from the correlation analysis described above). These standardized summed counts were then subjected to principal components analysis (PCA) to remove collinearity, with the principal component (PC) scores then standardized prior to entry into the ANN model (AM-ANN models).

Multiple ANN model-architectures were trialed using various numbers of retained PC scores (from 1 to 11 – the max number of AMs, and thus, PCs), and anywhere from 1 to 15 neurons, which add complexity to the ANN. Using methods similar to those described in Lee et al., (2017), ANNs were trained using Levenberg-Marquardt backpropagation, and validated internally using an early-stopping technique to prevent overfitting. An ensemble approach was used to quantify generalizability, whereby 50 models were trained (for each trialed model architecture), each with a different randomized training (70% of the dataset), internal validation (15% of the dataset, used for early stopping), and testing (another 15% of the

dataset) partitioning of the data. In the results below, we quantify model skill using R^2 values computed using the ensemble mean of the 50 different testing portions of the data – considered completely independent from the training/early-stopping of the model and thus, the best measure for generalizability.

In order to compare the efficacy of AM-based modeling with more-traditional dendroclimatological methods that often use temperature and precipitation, this entire process was repeated using standardized mean temperature and standardized summed precipitation data (from TerraClimate) over the same 12-month period (T&P-ANN models). Due to there only being 2 variables, no PCA was necessary for the ANN-T&P models, and a maximum of 2 input variables were entered into the model-architecture trials.

To quantify the importance of each individual AM in the multivariate model, we used Garson's method (Garson, 1991) for interpreting the input weights of ANNs. The Garson algorithm was run separately for each of the 50 member ANNs for a site and then averaged across the 50 models. The resulting output describes the importance of each individual input to the ANN; since the inputs were actually PC scores rather than raw AM counts, the averaged output was multiplied by the loadings/coefficients from the PCA described above (i.e. the PCA computed prior to ANN modeling). The resulting products of this multiplication were then ranked (1 to 11) at each location, yielding an estimate of how much weight an AM had in the ANN model ensemble at that site. We then average these ranks across all locations to get an estimate of the multivariate importance of different AMs in driving tree growth.

3. RESULTS AND DISCUSSION

While all 11 air masses were significantly correlated to TRW of at least one site, across all records, the Dry-Warm (DW), Dry (D), Warm (W) and Humid-Cool (HC) air masses were the most strongly and most frequently significantly (α=0.05) correlated to TRW, especially during seasons starting from the previous summer (i.e. JAS at Year -1) through the spring of the growth year (AMJ at Year 0; Table 1). For example, for Douglas-fir (PSME; n=111 sites), the most abundant tree species in the ITRDB, the median correlation between HC frequency and annual width was ρ = +0.2 to ρ = +0.3 for each of the aforementioned seasons, and close to ρ=-0.2 to ρ =-0.3 for DW frequency (Table 2). Of the 12 most abundant species in the dataset (those with at least 20 sites), European Beech (FASY, n=24) had the highest averaged correlation to AM frequencies, with ρ=-0.4 for DW air masses and ρ=+0.4 for HC air masses in the summer prior to growth (Table 3). Across all records in the database, the Humid (H) and Cool (C) air masses also played relatively large roles in these seasons, while transitional AMs (CFP and WFP), DC, and HW were not significantly correlated with TRW at most sites. The single most 'important' season (irrespective of the individual AMs) in determining TRW was generally spring in the growth year (i.e. AMJ at Year 0), suggesting some potential for using spring synoptic conditions to forecast growth for the year.

As an indicator of the ubiquity of AM-TRW relationships, every site (n=939) had at least one AM in one season with an absolute correlation of $|\rho| > 0.3$, and over 99% (934 of 939) of locations had at least one statistically significant (α=0.05) relationship to an AM in at least one season. Moreover, each of the 11 air masses had at least one site with an absolute

correlation of $|\rho| \geq 0.5$, with many exhibiting least $|\rho| > 0.6$, and some as high as $|\rho| > 0.8$. Using a similar air mass classification (the Spatial Synoptic Classification; Sheridan, 2002), Senkbeil et al. (2007) found similar correlations with a hot and dry air mass (significantly negative) and a humid and mild air mass (significantly positive) and tree rings along the Gulf coast of the United States.

Since individual AM frequency in a season will, by definition, be cross-correlated with the other AM frequencies to some degree (i.e. as one AM increases in seasonal frequency, another AM must simultaneously decrease), the multivariate perspective of the ANN models are also necessary to interpret predictability of TRW from AM frequencies. Overall, GWTC2 air masses explained a substantial amount of variability in global TRW data (mean = 28%, range 7% to 78%), including explaining at least 40% of the annual growth variability in TRW at 156 of 939 sites (Table 4), and over 60% of the variability at 22 of those sites. For one record – a Douglas-fir in Arizona, USA – the AM-only model explained 78% of TRW variability in this dry location.

The AM-based ANN models often explained more variability than T&P-ANN models (Table 4; Figure 3). Of the 939 sites, the R^2 of the AM-only ANN model was better than that of the T&P-ANN model in 59% of the *individual* records, and was better for 62% of the 144 different *species* represented in the dataset. In fact, for the 24 tree species that had at least 10 individual records in the dataset, the average R^2 of the AM-only ANN models was superior to that of the T&P-ANN models for 20 (83%) of them. However, generally the AM-ANN and T&P-ANN models performed best at the same locations, especially in the southwestern US. These results are comparable to semiempirical temperature- and precipitation-based tree-ring models that explained, on average, ~40% of the variance in TRW in dry ecoregions and <20% of the variance in moist ecoregions in the United States (Dannenberg, 2021). The AM-ANN models were markedly better than the T&P-ANN models in Alaska and northwestern Canada, along with many of the sites in Asia.

For each AM, the variable importance from the ANN models mostly revealed quite similar results as those found in the univariate correlation analysis. The largest difference was the relatively high importance of the Dry-Cool (DC) AM in the ANN model: while it was the ninth most-often significantly correlated AM in the univariate analysis, it rose to first in importance of the 11 AMs in the ANN models (Table 5). Also noteworthy is the slight *decreased* importance of DW – falling from first to fourth-most important AM in the multivariate analysis. The Warm AM also had less importance in the multivariate models compared to the univariate analysis, dropping from third to sixth in importance. These differences indicate that when included in a multivariate model, the DW and W air masses are likely providing some duplicate information that is already captured by the other AMs, decreasing their importance relative to the less-strongly cross-correlated AMs that contain more unique information. Indeed, when examining frequency correlations between the core AMs (not shown), the DW and W air masses are the most strongly correlated to the frequency of other AMs, while DC is the second least correlated to the other core-AMs.

The way a particular AM relates to tree growth is somewhat dependent on mean annual temperature (MAT) of the site (Table 6, Figures 4-5). There is a direct positive association

between MAT and the importance of the HC, Cool, and to a lesser extent, Humid AMs: the warmer the MAT of the site, the more important the frequency of these three AMs. By contrast, there is a large inverse relationship between mean temperature and the DW, Warm, and Dry AMs, meaning that the warmer the site is, the more inverse the relationship between these AM frequencies and tree growth. Mean annual precipitation was less important overall than MAT in this regard: only the Warm (positive) and the HC (negative) in AMJ Year0 have a correlation with MAP greater than ρ = +/-0.2. When correlating R^2 values from the ANN models with MAT and MAP, the ability of the GWTC2 on the whole to explain TRW variability (using ANN models) was also significantly related to MAT of the site (ρ=0.09; p=0.008), but was not significantly related to MAP. This said, the *difference* between R^2 for AM-ANNs and T&P-ANNs was significantly directly related to MAP (ρ=0.1; p<0.001), indicating that the AM-ANNs generally performed slightly better than T&P-ANNs in wetter sites (Figure 6).

4. SUMMARY AND CONCLUSIONS

This research presents an initial examination of the ability of multivariate surface air masses to impact tree growth. To our knowledge no such prior analysis has explored this relationship at a global scale, and certainly not with the GWTC2. We found strong relationships between annual tree-ring widths and the frequencies of different air masses, with these relationships being strongest during the 12-month period beginning in July of the prior year and ending in June of the year of growth. These relationships were sufficiently strong that empirical models based solely on AM frequencies outperformed temperature- and precipitation-based models (which are more commonly used for tree-ring modeling) at about 60% of sites and for about 60% of species. Among the 11 air masses, the Dry-Warm (DW) AM in the year of growth was the most strongly and frequently correlated with TRW in the univariate analysis, and on average was the third-most important of the AMs in the multivariate models. The Humid-Cool, Warm, and Dry AMs also played important roles at many sites, while the Dry-Cool AM added unique information into the multivariate models and was the most important AM on average using the AM-ANN models.

While this research demonstrates significant potential for prediction of growth based on synoptic-scale climate, and while the tree-ring record does represent multiple climate regions across the globe, the vast majority of sites come primarily from North America (especially the US) and (to a lesser degree) Europe and parts of Asia, with only a handful of locations in the tropics and the Southern Hemisphere. Due to the temporal limits of the GWTC2 dataset, this research was also limited to a fairly short time-span (1979-2020 or shorter, depending on the length of the tree-ring record at each site), especially relative to the life cycle of many tree species. Further, while some species/sites show strong relationships to AM frequencies, there is still considerable variability in these relationships from site to site. Therefore, it should not be assumed that the entire range of environmental conditions across all individual members of a species is representatively sampled here. Relative to their global abundance, the ITRDB tends to oversample old, coniferous trees in climatically-extreme environments to maximize their utility for climate reconstruction (Klesse et al., 2018; Zhao et al., 2018), and it is therefore likely that the sites used in this analysis are not fully representative of global forest ecosystems.

Despite these limitations, this research shows that not only is tree growth impacted by multivariate, synoptic-scale atmospheric conditions, but moreover, for many species and locations, multivariate air masses are *better* indicators of tree growth than local temperature and precipitation alone. There has been a keen interest recently in ecological forecasting (Dietze et al., 2018; Luo et al., 2011) and the impacts of antecedent abiotic factors on plant stress (Dannenberg et al., 2019, 2020; Dannenberg & Wise, 2016; Earles et al., 2018; Jiao et al., 2022; Kannenberg et al., 2019b; Ogle et al., 2014; Peltier et al., 2018). In particular, knowing the potential for tree growth or tree stress in the upcoming months based upon the conditions up to 12 months prior could aid in forecasts for wildfire vulnerability and widespread tree mortality. This research suggests that, compared to just using recent temperature and precipitation records, air masses offer the potential to improve such predictions. Moreover, the TRW/AM relationship could work in both directions: the centuries-long proxy records stored in tree rings may allow long-term reconstructions of air masses back several hundred years. Such reconstructions would allow quantification and contextualization of recent trends in AM frequencies (e.g., Lee, 2020a; Lee & Sheridan, 2018; Petrou et al. 2022) that are not achievable from instrumental records alone.

ACKNOWLEDGEMENTS AND DATA AVAILABILITY

MPD was supported by the National Science Foundation's Paleo Perspectives on Climate Change (P2C2) program (grant AGS-2001753). All analyses were conducted using MatLab, version 2019a and later. The final/trimmed climate and tree-ring data sets used in this research and the trained artificial neural networks (ANNs) are preserved in Matlab formatted data files (.mat), and are available in the Mendeley Data repository at: https://data.mendeley.com/drafts/5s5xykzwyd; Lee and Dannenberg, 2022). Raw tree-ring data are available through NOAA's National Centers for Environmental Information and the World Data Center for Paleoclimatology (https://www.ncdc.noaa.gov/data-access/paleoclimatology-data/datasets/treering), while raw GWTC2 air mass data are available at: https://www.personal.kent.edu/~cclee/gwtc2global.html, and raw TerraClimate data are available at: https://www.climatologylab.org/terraclimate.html.

REFERENCES

Abatzoglou, J. T., Dobrowski, S. Z., Parks, S. A., & Hegewisch, K. C. (2018). TerraClimate, a high-resolution global dataset of monthly climate and climatic water balance from 1958-2015. Scientific Data, 5, 170191. https://doi.org/10.1038/sdata.2017.191.

Anchukaitis, K. J., Evans, M. N., Hughes, M. K., & Vaganov, E. A. (2020). An interpreted language implementation of the Vaganov–Shashkin tree-ring proxy system model. Dendrochronologia, 60, 125677. https://doi.org/10.1016/j.dendro.2020.125677.

Bunn, A. G. (2008). A dendrochronology program library in R (dplR). Dendrochronologia, 26(2), 115–124. https://doi.org/10.1016/j.dendro.2008.01.002.

Cook, E. R., & Peters, K. (1981). The smoothing spline: a new approach to standardizing forest interior tree-ring width series for dendroclimatic studies. Tree-Ring Bulletin, 41, 45–53.

Cook, E. R., Meko, D. M., Stahle, D. W., & Cleaveland, M. K. (1999). Drought reconstructions for the continental United States. Journal of Climate, 12, 1145–1162.

Cook, E. R., Seager, R., Kushnir, Y., Briffa, K. R., Büntgen, U., Frank, D., … Zang, C. (2015). Old World megadroughts and pluvials during the Common Era. Science Advances, 1(10), e1500561. https://doi.org/10.1126/sciadv.1500561.

Dannenberg, M. P. (2021). Modeling tree radial growth in a warming climate: Where, when, and how much do potential evapotranspiration models matter? Environmental Research Letters, 16(8). https://doi.org/10.1088/1748-9326/ac1292.

Dannenberg, M. P. & E. K. Wise (2016). Seasonal climate signals from multiple tree ring metrics: A case study of Pinus ponderosa in the upper Columbia River Basin. Journal of Geophysical Research: Biogeosciences, 121, 1178-1189.

Dannenberg, M. P., & Wise, E. K. (2017). Shifting Pacific storm tracks as stressors to ecosystems of western North America. Global Change Biology, 23(11), 4896–4906. https://doi.org/10.1111/gcb.13748.

Dannenberg, M. P., Song, C., Wise, E. K., Pederson, N., & Bishop, D. A. (2020). Delineating Environmental Stresses to Primary Production of U.S. Forests From Tree Rings: Effects of Climate Seasonality, Soil, and Topography. Journal of Geophysical Research: Biogeosciences, 125(2), 1–16. https://doi.org/10.1029/2019JG005499.

Dannenberg, M. P., Wise, E. K., & Smith, W. K. (2019). Reduced tree growth in the semiarid United States due to asymmetric responses to intensifying precipitation extremes. Science Advances, 5(10), eaaw0667. https://doi.org/10.1126/sciadv.aaw0667.

Dietze, M. C., A. Fox, L. M. Beck-Johnson, J. L. Betancourt, M. B. Hooten, C. S. Jarnevich, T. H. Keitt, M. A. Kenney, C. M. Laney, L. G. Larsen, H. W. Loescher, C. K. Lunch, B. C. Pijanowski, J. T. Randerson, E. K. Read, A. T. Tredennick, R. Vargas, K. C. Weathers, & E. P. White (2018). Iterative near-term ecological forecasting: Needs, opportunities, and challenges. Proceedings of the National Academy of Sciences USA, 115, 1424-1432.

Earles, J. M., Stevens, J. T., Sperling, O., Orozco, J., North, M. P., & Zwieniecki, M. A. (2018). Extreme mid-winter drought weakens tree hydraulic-carbohydrate systems and slows growth. New Phytologist, 219(1), 89–97. https://doi.org/10.1111/nph.15136

Garson, G.D., 1991. Interpreting neural-network connection weights. AI Expert, 6(4), pp.46-51.

Hirschboeck, K. K., Ni, F., Wood, M. L., & Woodhouse, C. A. (1996). Synoptic dendroclimatology: overview and prospectus. In J. S. Dean, D. M. Meko, & T. W. Swetnam

(Eds.), Tree-Rings, Environment and Humanity: Proceedings of the International Conference (pp. 205–223). Tucson, AZ: The University of Arizona.

Hondula, D.M., Vanos, J.K. and Gosling, S.N., 2014. The SSC: a decade of climate–health research and future directions. International journal of biometeorology, 58(2), pp.109-120.

Hudson, A. R., Alfaro-Sanchez, R., Babst, F., Belmecheri, S., Moore, D. J. P., & Trouet, V. (2019). Seasonal and synoptic climatic drivers of tree growth in the Bighorn Mountains, WY, USA (1654–1983 CE). Dendrochronologia, 58(August), 125633. https://doi.org/10.1016/j.dendro.2019.125633.

Jiao, W., L. Wang, H. Wang, M. Lanning, Q. Chang, & K. A. Novick (2022). Comprehensive quantification of the responses of ecosystem production and respiration to drought time scale, intensity and timing in humid environments: A FLUXNET synthesis, Journal of Geophysical Research: Biogeosciences, 127, e2021JG006431.

Kannenberg, S. A., Maxwell, J. T., Pederson, N., D'Orangeville, L., Ficklin, D. L., & Phillips, R. P. (2019a). Drought legacies are dependent on water table depth, wood anatomy and drought timing across the eastern US. Ecology Letters, 22(1), 119–127. https://doi.org/10.1111/ele.13173.

Kannenberg, S. A., Novick, K. A., Alexander, M. R., Maxwell, J. T., Moore, D. J. P., Phillips, R. P., & Anderegg, W. R. L. (2019b). Linking drought legacy effects across scales: From leaves to tree rings to ecosystems. Global Change Biology, 25(9), 2978–2992. https://doi.org/10.1111/gcb.14710

Klesse, S., R. J. DeRose, C. H. Guiterman, A. M. Lynch, C. D. O'Connor, J. D. Shaw, & M. E. K. Evans (2018), Sampling bias overestimates climate change impacts on forest growth in the southwestern United States, Nature Communications, 9, 5336.

Labosier, C.F., Frauenfeld, O.W., Quiring, S.M. and Lafon, C.W., 2015. Weather type classification of wildfire ignitions in the central Gulf Coast, United States. International Journal of Climatology, 35(9), pp.2620-2634.

Lee, C.C., 2015a. A systematic evaluation of the lagged effects of spatiotemporally relative surface weather types on wintertime cardiovascular-related mortality across 19 US cities. International journal of biometeorology, 59(11), pp.1633-1645.

Lee, C.C., 2015b. The development of a gridded weather typing classification scheme. International Journal of Climatology, 35(5), pp.641-659.

Lee, C.C. and Dannenberg, M.P. (2022), "Air Masses and Tree Rings", Mendeley Data, V1, DOI: 10.17632/5s5xykzwyd.1.

Lee, C.C., Sheridan, S.C., Barnes, B.B., Hu, C., Pirhalla, D.E., Ransibrahmanakul, V. and Shein, K., 2017. The development of a non-linear autoregressive model with exogenous input (NARX)

to model climate-water clarity relationships: reconstructing a historical water clarity index for the coastal waters of the southeastern USA. Theoretical and Applied Climatology, 130(1), pp.557-569.

Lee, C.C., 2020a. Trends and Variability in Airmass Frequencies: Indicators of a Changing Climate. Journal of Climate, 33(19), pp.8603-8617.

Lee, C.C., 2020b. The gridded weather typing classification version 2: A global-scale expansion. International Journal of Climatology, 40(2), pp.1178-1196.

Lee, C.C. and Sheridan, S.C., 2018. Trends in weather type frequencies across North America. NPJ Climate and Atmospheric Science, 1(1), pp.1-7.

Luo, Y., K. Ogle, C. Tucker, S. Fei, C. Gao, S. LaDeau, J. S. Clark, & D. S. Schimel (2011). Ecological forecasting and data assimilation in a data-rich era. Ecological Applications, 21, 1429-1442.

Ogle, K., J. J. Barber, G. A. Barron-Gafford, L. P. Bentley, J. M. Young, T. E. Huxman, M. E. Loik, D. T. Tissue (2014). Quantifying ecological memory in plant and ecosystem processes. Ecology Letters, 18, 221-235.

Peltier, D. M. P., Barber, J. J., & Ogle, K. (2018). Quantifying antecedent climatic drivers of tree growth in the Southwestern US. Journal of Ecology, 106(2), 613–624. https://doi.org/10.1111/1365-2745.12878.

Petrou, I., Kassomenos, P. and Lee, C.C., 2022. Trends in air mass frequencies across Europe. Theoretical and Applied Climatology, pp.1-16.

Schultz, J.A. and Neuwirth, B., 2012. A new atmospheric circulation tree-ring index (ACTI) derived from climate proxies: Procedure, results and applications. Agricultural and forest meteorology, 164, pp.149-160.

Seim, A., Schultz, J. A., Leland, C., Davi, N., Byambasuren, O., Liang, E., … Pederson, N. (2017). Synoptic-scale circulation patterns during summer derived from tree rings in mid-latitude Asia. Climate Dynamics, 49(5–6), 1917–1931. https://doi.org/10.1007/s00382-016-3426-7.

Senkbeil, J. C., Rodgers, J. C., & Sheridan, S. C. (2007). The sensitivity of tree growth to air mass variability and the Pacific Decadal Oscillation in coastal Alabama. International Journal of Biometeorology, 51(6), 483–491. https://doi.org/10.1007/s00484-007-0087-6.

Sheridan, S.C., 2002. The redevelopment of a weather-type classification scheme for North America. International Journal of Climatology: A Journal of the Royal Meteorological Society, 22(1), pp.51-68.

Tolwinski-Ward, S. E., Anchukaitis, K. J., & Evans, M. N. (2013). Bayesian parameter estimation and interpretation for an intermediate model of tree-ring width. Climate of the Past, 9(4), 1481–1493. https://doi.org/10.5194/cp-9-1481-2013.

Tolwinski-Ward, S. E., Evans, M. N., Hughes, M. K., & Anchukaitis, K. J. (2011). An efficient forward model of the climate controls on interannual variation in tree-ring width. Climate Dynamics, 36(11–12), 2419–2439. https://doi.org/10.1007/s00382-010-0945-5.

Trouet, V., Babst, F., & Meko, M. (2018). Recent enhanced high-summer North Atlantic Jet variability emerges from three-century context. Nature Communications, 9(1), 180. https://doi.org/10.1038/s41467-017-02699-3.

Williams, A. P., Allen, C. D., Macalady, A. K., Griffin, D., Woodhouse, C. A., Meko, D. M., … McDowell, N. G. (2013). Temperature as a potent driver of regional forest drought stress and tree mortality. Nature Climate Change, 3(3), 292–297. https://doi.org/10.1038/nclimate1693.

Wilson, R., Anchukaitis, K., Briffa, K. R., Büntgen, U., Cook, E., D'Arrigo, R., … Zorita, E. (2016). Last millennium northern hemisphere summer temperatures from tree rings: Part I: The long term context. Quaternary Science Reviews, 134, 1–18. https://doi.org/10.1016/j.quascirev.2015.12.005.

Wise, E. K. (2010). Tree ring record of streamflow and drought in the upper Snake River. Water Resources Research, 46, W11529. https://doi.org/10.1029/2010WR009282.

Wise, E. K., & Dannenberg, M. P. (2014). Persistence of pressure patterns over North America and the North Pacific since AD 1500. Nature Communications, 5, 4912.

Wise, E. K., & Dannenberg, M. P. (2017). Reconstructed storm tracks reveal three centuries of changing moisture delivery to North America. Science Advances, 3(6), e1602263. https://doi.org/10.1126/sciadv.1602263.

Woodhouse, C. A., & Kay, P. A. (1990). The use of tree-ring chronologies to show spatial and temporal changes in an air mass boundary. Physical Geography, 11(2), 172–190. https://doi.org/10.1080/02723646.1990.10642401.

Zhao, S., N. Pederson, L. D'Orangeville, J. HilleRisLambers, E. Boose, C. Penone, B. Bauer, Y. Jiang, & R. D. Manzanedo (2018), The International Tree-Ring Data Bank (ITRDB) revisited: Data availability and global ecological representativity, Journal of Biogeography, 46(2), 355-368.

TABLES

Table 1. *Percentage of the n=939 retained TRW records that had significant (α=0.05) rank-correlations between TRW and air masses (columns) for each season (rows). Darker reds depict higher percentages.*

% Sig RHO		HC	H	HW	C	S	W	DC	D	DW	CFP	WFP
YEAR -1	JFM	6%	6%	4%	8%	7%	8%	6%	8%	9%	5%	5%
	AMJ	8%	9%	5%	8%	7%	8%	5%	13%	12%	6%	4%
	JAS	19%	12%	8%	11%	6%	17%	6%	14%	21%	7%	5%
	OND	12%	12%	7%	12%	5%	9%	6%	10%	14%	6%	5%
YEAR 0	JFM	12%	13%	7%	12%	11%	14%	8%	15%	16%	6%	7%
	AMJ	19%	17%	7%	19%	10%	19%	6%	17%	23%	6%	5%
	JAS	7%	10%	8%	7%	8%	12%	9%	13%	17%	5%	7%
	OND	9%	5%	6%	7%	4%	6%	5%	5%	7%	6%	6%

Table 2. *Mean spearman rank correlation (ρ) between AMs (columns) and TRW for each season (rows) for the n=111 retained records of Douglas-Fir (PSME). Darker blues depict stronger negative correlations, darker reds depict stronger positive correlations.*

Mean Rho		HC	H	HW	C	S	W	DC	D	DW	CFP	WFP
YEAR -1	JFM	0.04	0.03	0.04	0.07	-0.02	-0.03	0.09	-0.08	-0.05	-0.01	0.02
	AMJ	0.15	0.19	0.02	-0.01	0.12	-0.07	-0.06	-0.18	-0.15	-0.10	0.03
	JAS	0.29	0.07	-0.07	0.22	0.08	-0.25	0.06	-0.14	-0.31	0.04	-0.01
	OND	0.28	0.27	0.03	0.21	0.06	-0.21	-0.07	-0.22	-0.26	-0.05	-0.02
YEAR 0	JFM	0.20	0.17	0.09	0.16	0.07	-0.12	-0.06	-0.20	-0.20	-0.08	-0.05
	AMJ	0.31	0.22	-0.08	0.21	0.15	-0.29	0.00	-0.21	-0.32	0.02	0.04
	JAS	0.05	0.03	-0.06	0.11	0.11	-0.16	0.07	0.00	-0.22	0.03	-0.01
	OND	0.07	0.08	0.05	0.08	0.01	-0.09	-0.02	-0.11	-0.08	-0.02	-0.05

Table 3. *Same as Table 2, except for the n=24 retained records of European Beech (FASY).*

Mean Rho		HC	H	HW	C	S	W	DC	D	DW	CFP	WFP
YEAR -1	JFM	0.16	-0.25	-0.05	0.14	-0.11	-0.17	0.15	-0.03	-0.05	-0.01	0.04
	AMJ	0.12	0.09	0.16	0.00	-0.03	-0.08	0.00	-0.14	-0.13	-0.01	0.07
	JAS	0.41	0.31	-0.04	0.32	0.10	-0.34	0.04	-0.36	-0.44	-0.11	0.08
	OND	0.03	-0.08	0.04	0.00	0.12	-0.04	-0.06	-0.21	-0.19	-0.03	0.09
YEAR 0	JFM	0.09	-0.07	-0.11	0.01	0.02	-0.06	0.15	-0.06	-0.06	0.20	-0.05
	AMJ	0.08	0.24	0.21	0.07	0.09	-0.18	-0.04	-0.18	-0.28	0.01	0.06
	JAS	0.13	0.21	0.06	-0.12	0.05	-0.06	-0.06	-0.28	-0.17	0.02	0.01
	OND	-0.02	-0.06	0.07	-0.02	-0.07	0.11	0.07	-0.12	-0.03	-0.04	0.01

Table 4. *Left: the mean percent of TRW variability explained (R^2) by the AM-only ANN model (AM) and the temperature and precipitation (T&P) ANN model for the 12 tree species with at least 20 retained records in the database. Right: the count (out of n=939) of individual records with explained variability (R^2) above different thresholds for the AM and T&P ANN models.*

Species	n	AM	T&P
'PSME'	111	36%	35%
'PCGL'	57	26%	25%
'PIPO'	48	32%	33%
'PISY'	38	26%	21%
'PCAB'	33	27%	20%
'TSME'	25	29%	20%
'FASY'	24	33%	30%
'LADE'	24	29%	21%
'LASI'	23	24%	20%
'PCMA'	22	23%	17%
'QUMA'	22	27%	25%
'CHTH'	21	23%	18%

R^2>	AM	T&P
30%	355	305
40%	156	152
50%	57	50
60%	22	10
70%	4	1

Table 5. *Estimated rank of importance of each AM in the AM-ANN models (ANN) versus the univariate correlation models (CORR; 1=most important of the 11 AMs).*

	RANK	
AM	**ANN**	**CORR**
HC	3	4
H	5	5
HW	9	8
C	8	6
S	7	7
W	6	3
DC	1	9
D	2	2
DW	4	1
CFP	10	10
WFP	11	11

Table 6. *Top: the spatial Spearman rank correlation (n=939) between mean annual temperature (MAT) of a site and the Spearman rank correlation between TRW and AM frequencies at that site. Bottom: the same, except for mean annual precipitation (MAP) of each site.*

MAT		HC	H	HW	C	S	W	DC	D	DW	CFP	WFP
YEAR -1	JFM	0.15	-0.07	-0.02	0.24	-0.07	-0.07	0.08	-0.08	-0.22	0.10	0.04
	AMJ	0.04	-0.03	-0.01	0.13	0.08	-0.15	0.02	-0.16	-0.12	0.06	0.04
	JAS	-0.07	-0.10	-0.06	0.13	-0.02	-0.03	0.07	0.06	0.00	0.04	-0.01
	OND	0.16	0.16	0.01	0.23	0.07	-0.22	0.00	-0.26	-0.31	0.09	-0.03
YEAR 0	JFM	0.20	0.19	0.07	0.17	0.11	-0.08	-0.16	-0.29	-0.21	-0.02	-0.07
	AMJ	0.24	0.07	-0.12	0.36	0.15	-0.27	0.11	-0.15	-0.36	0.10	0.14
	JAS	0.16	0.10	-0.11	0.23	0.13	-0.22	0.16	-0.10	-0.29	0.12	0.02
	OND	0.02	0.11	0.05	0.09	-0.03	-0.03	0.03	-0.16	-0.12	0.08	-0.16

MAP		HC	H	HW	C	S	W	DC	D	DW	CFP	WFP
YEAR -1	JFM	0.03	-0.07	0.04	0.11	-0.06	0.02	0.00	-0.02	-0.11	0.09	0.06
	AMJ	-0.13	-0.13	-0.03	0.03	-0.01	0.05	0.01	0.00	0.06	0.14	0.09
	JAS	-0.18	-0.08	0.00	-0.06	-0.07	0.12	-0.01	0.14	0.13	0.01	0.06
	OND	-0.20	-0.09	-0.05	-0.12	0.04	0.07	0.01	0.09	0.07	0.06	-0.05
YEAR 0	JFM	-0.17	-0.02	-0.01	-0.12	-0.06	0.21	-0.05	-0.01	0.18	0.07	-0.09
	AMJ	-0.21	-0.19	0.03	-0.11	-0.07	0.22	-0.01	0.18	0.08	0.03	0.02
	JAS	-0.12	0.11	0.01	-0.04	-0.12	0.12	-0.08	0.02	0.04	0.00	0.03
	OND	-0.05	-0.05	-0.06	0.04	-0.12	0.09	0.05	-0.02	0.00	0.13	-0.02

FIGURES

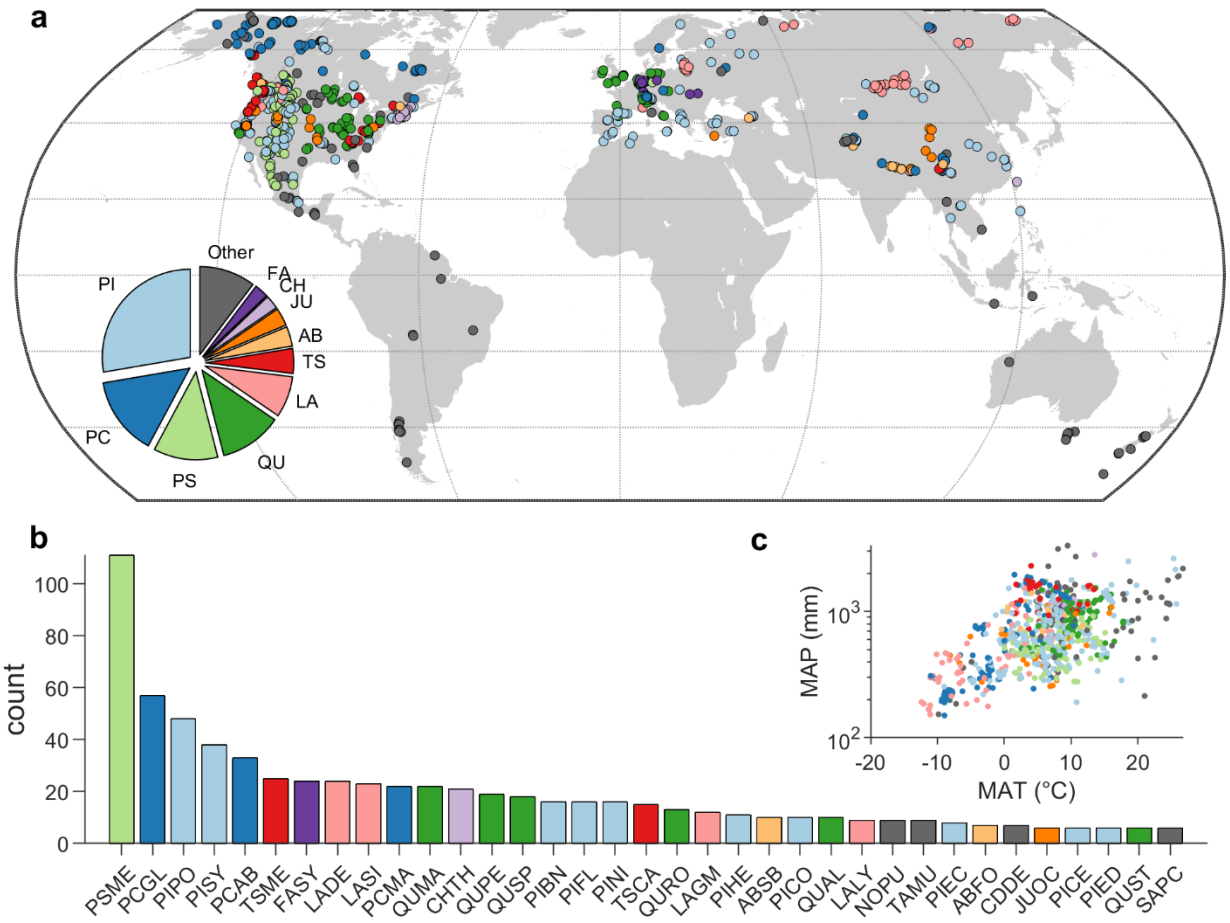

Figure 1. (a) Distribution of the 939 tree-ring sites used in this study, from the International Tree Ring Data Bank (ITRDB). Colors indicate the genus sampled at each site, with total proportions belonging to each genus shown in the pie chart. [PI: *Pinus*, PC: *Picea*, PS: *Pseudotsuga*, QU: *Quercus*, LA: *Larix*, TS: *Tsuga*, AB: *Abies*, JU: *Juniperus*, CH: *Chamaecyparis*, FA: *Fagus*] (b) Histogram of the number of sites belonging to the 35 most common species represented in the dataset (species with 5 or fewer sites are not shown), with colors corresponding to the genera shown in (a). Full names and numbers of sites for each species are shown in Supplementary Table S#. (c) Mean annual temperature (MAT) and precipitation (MAP) of the tree-ring sites from TerraClimate, with precipitation on a log scale and colors corresponding to the genera shown in (a).

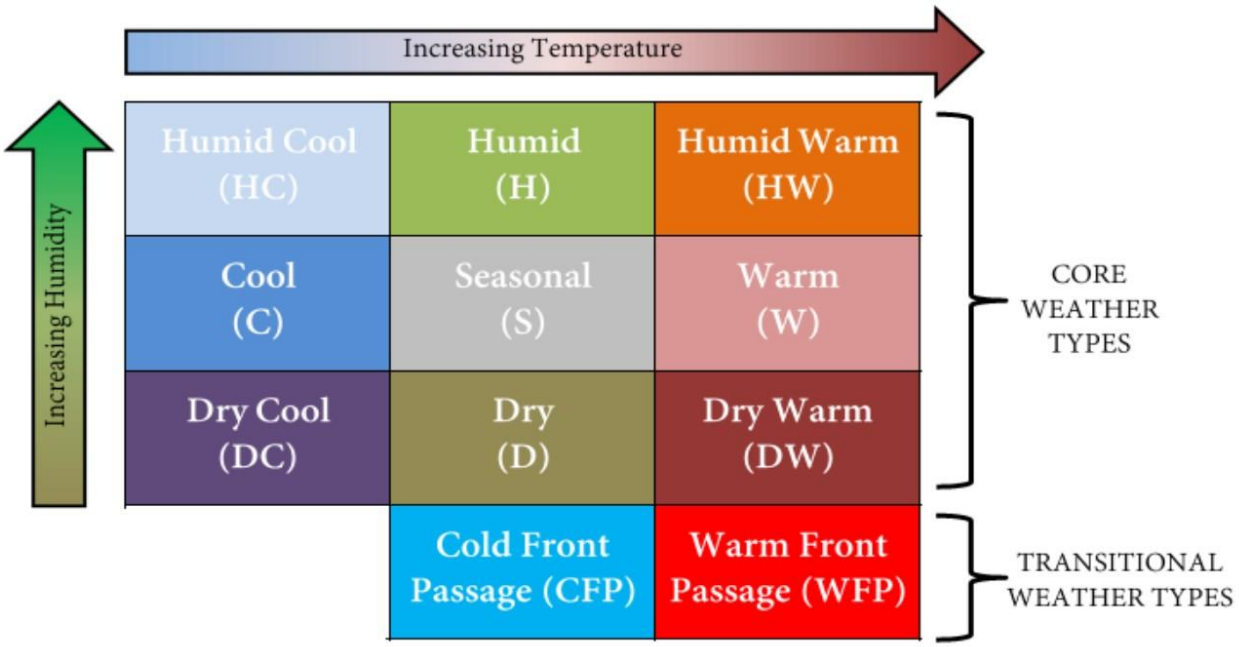

637
638 **Figure 2** – The GWTC2 air masses.
639
640

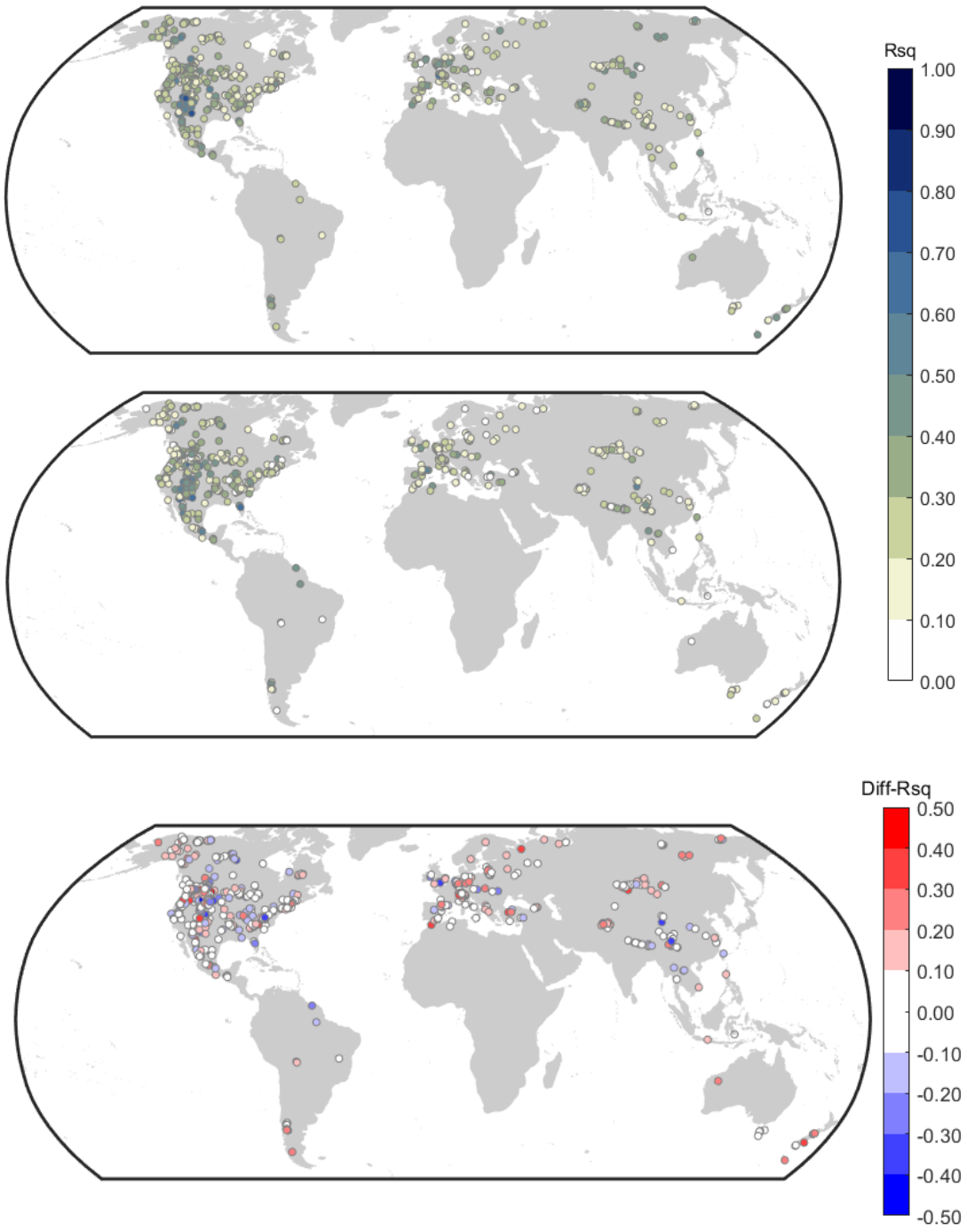

Figure 3. Mapped ANN model performance. R-squared (R^2) values for the ANN models trained on AMs only (top), the T&P-ANN (middle), and the difference between the two model types (bottom; increasingly red colors indicate the AM-ANN is better than the T&P-ANN model, increasingly blue colors indicate the T&P-ANNs are better than the AM-ANNs).

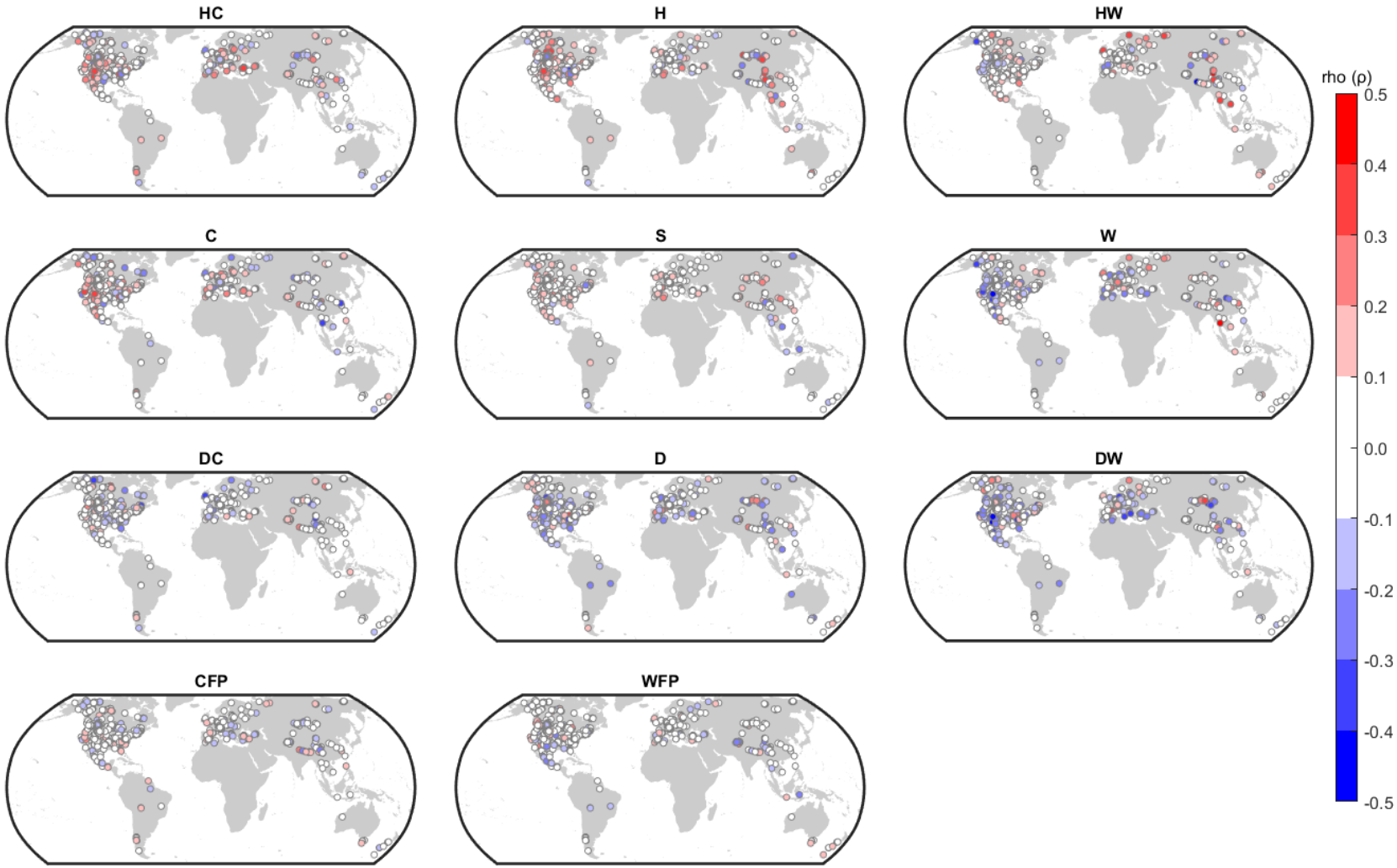

Figure 4. Average correlation of each AM with TRW at each tree-ring site. Each average correlation is the mean Spearman's rho (ρ) across the n=8 seasons in Year0 and Year-1 (i.e. the average of one of the columns in Table 2).

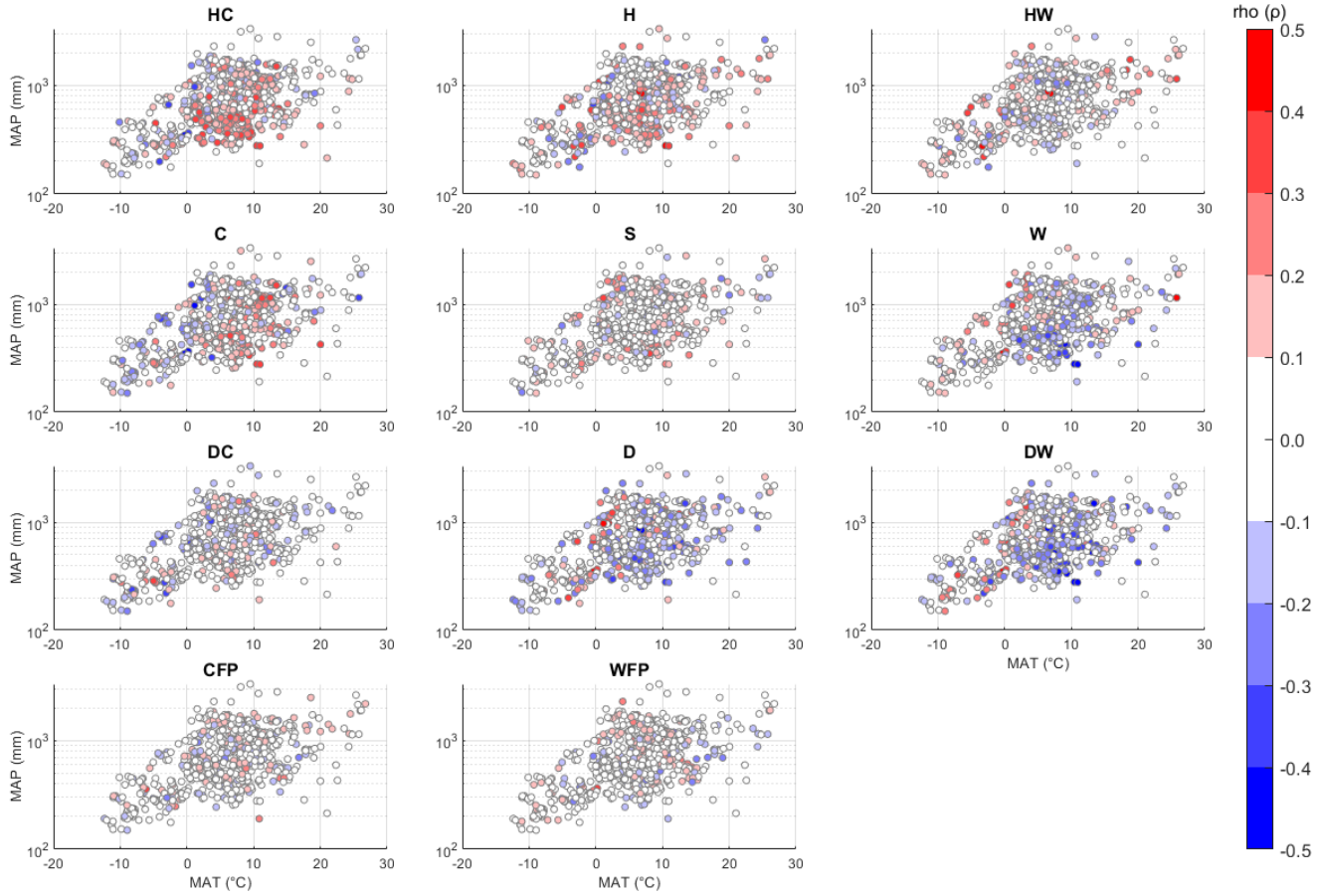

Figure 5. Relationships between MAP, MAT, and average correlation (ρ) between TRW and each AM. Red-to-blue coloring of the markers indicate the averaged correlation (across the n=8 seasons for Year0 and Year-1 of each AM), relative to mean annual temperature (MAT; x-axis) and mean annual precipitation (MAP, y-axis – log-scale) for each site.

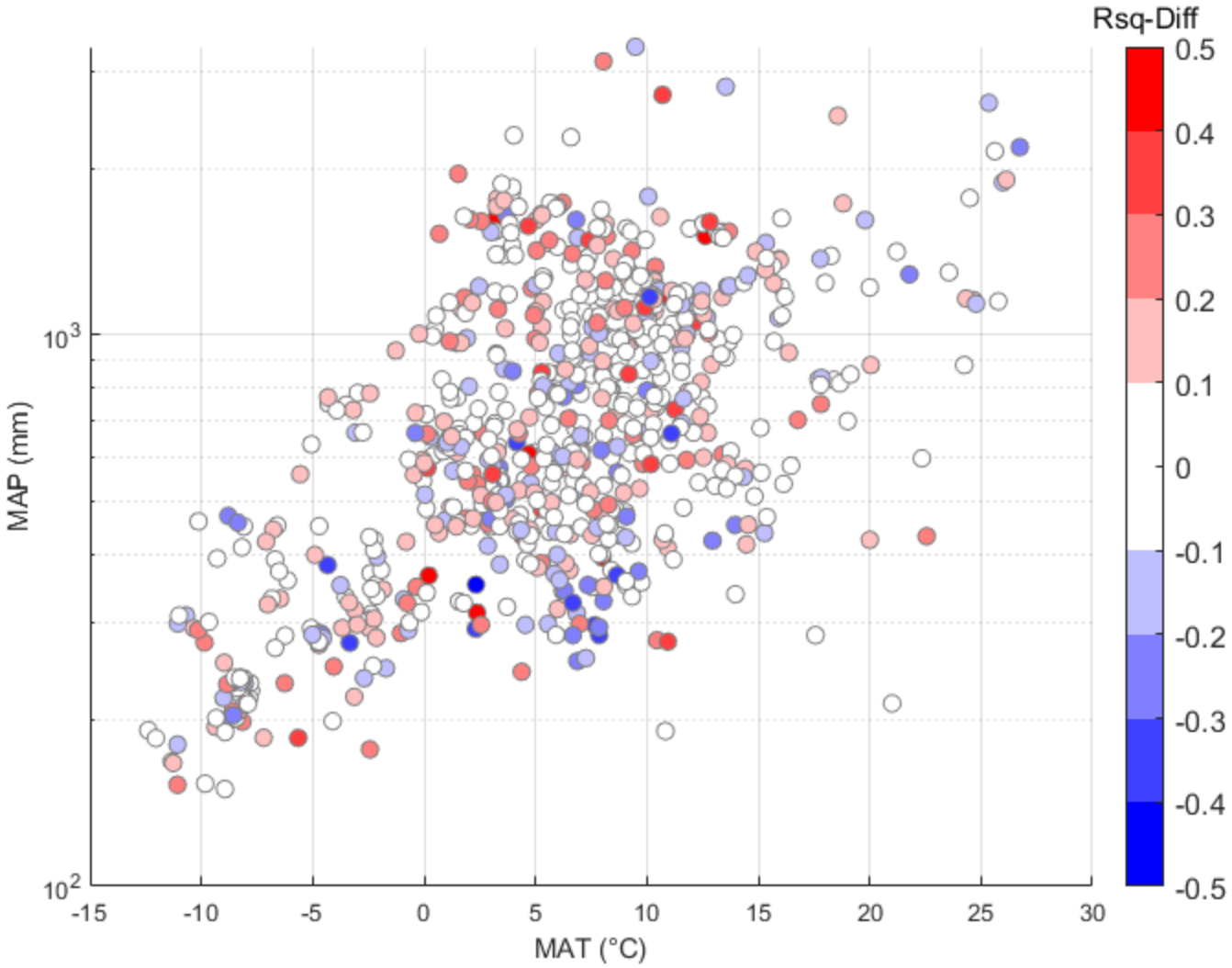

Figure 6. Difference in performance of AM-only ANN models vs. T&P-ANN models, by MAP (y-axis, log-scale) and MAT (x-axis) of each site. Colors represent the difference in R^2 values of the models, with positive values (reds) indicating better model performance of the AM-only ANN model.